The influence of the substitution of Te for Se on the photoconductive properties of $In_2Se_{3-x}Te_{3x}$ thin films

2001 J. Phys.: Condens. Matter 13 1839

(http://iopscience.iop.org/0953-8984/13/9/307)

INSTITUTE OF PHYSICS PUBLISHING JOURNAL OF PHYSICS: CONDENSED MATTER

J. Phys.: Condens. Matter **13** (2001) 1839–1850 www.iop.org/Journals/cm PII: S0953-8984(01)17768-4

The influence of the substitution of Te for Se on the photoconductive properties of $In_2Se_{3-x}Te_{3x}$ thin films

H El Maliki[1], S Marsillac[1], J C Bernède[1], E Faulques[2] and J Wery[2]

[1] Equipe Couches Minces et Matériaux Nouveaux, EPSE FSTN, 2 rue de la Houssinière, BP 92208, 44322 Nantes Cédex 3, France
[2] LPC IMN, BP 92208, 44322 Nantes Cédex 3, France

Received 5 October 2000, in final form 18 January 2001

Abstract

Thin films of $In_2Se_{3-3x}Te_{3x}$ compounds have been synthesized by annealing, in constant argon flow, a multilayer structure of indium, selenium and tellurium, sequentially deposited. The films have been characterized by x-ray diffraction (XRD), electron microprobe analysis and x-ray photoelectron spectroscopy (XPS) measurements. These studies have shown that the thin films after annealing are stoichiometric with In at.%/(Se + Te) at.% $= 2/3$. Qualitative XPS analyses have provided evidence that the surface of the films is chalcogen deficient. XRD measurements have shown that the thin films are crystallized in the hexagonal structure of γ-In_2Se_3. The transmission curves obtained by optical measurements show that the absorption threshold is about 1.8 eV when x varies between 0 and 0.25. The photoconductivity measurements have shown that the presence of some at.% of Te (0.8 at.%–8 at.%) improves the photocurrent of the films. The photocurrent is increased by more than five orders of magnitude in the presence of 8 at.% of Te. These properties make $In_2Se_{3-3x}Te_{3x}$ compounds very interesting materials as regards use as absorbers in thin-film solar cells.

1. Introduction

The most effective thin-film solar cells are based on Cu(In, Ga)Se_2 layers with a band gap of 1.2 eV for a Ga/(Ga + In) ratio of about 0.25. The use of such absorbing layers allows one to achieve energy-conversion efficiencies exceeding 17% [1].

However, materials with a broad band gap, 1.5 eV and even more, should induce corresponding higher open-circuit voltage in the solar cells and have a series of advantages [2]:

- the loss of the open-circuit voltage with increasing temperature is lower for wide-gap materials;
- the ohmic losses are minimized due to the lower current density.

γ-In_2Se_3 with a band gap of 1.8 eV [3] is a possible candidate for application as an absorber layer in wide-gap thin-film solar cells. However, γ-In_2Se_3-based thin-film solar cells fail to

overcome a limitation to just a few per cent efficiency. The most critical drawback of γ-In_2Se_3 is its poor conductivity [4]. One possibility for decreasing this resistivity is to introduce some Te in the films in order to obtain $In_2Se_{3-3x}Te_{3x}$. Such a process has proved very successful in the case of $CdSe_{1-x}Te_x$ films [5]. This article describes results obtained on such ternary compounds.

2. Thin-film preparation and characterization

2.1. Film preparation

All of the depositions were done in a vacuum better than 10^{-5} Pa. The substrates used were soda-lime glass. The glass substrates were degreased with standard solvents and ultrasound and then rinsed in deionized water. The $In_2Se_{3-3x}Te_{3x}$ samples were obtained by a solid-state reaction, induced by annealing, between In, Se and Te constituents sequentially deposited in thin-film form. The In, Se and Te have purity of 99.999%. The In, Se and Te layers were deposited sequentially; they were deposited by alternating evaporation from a resistance-heated tungsten crucible. The evaporation rates and film thicknesses were measured *in situ* by a hf quartz monitor. The evaporation rates were 0.7 nm s^{-1} for In, 0.3 nm s^{-1} for Se and 0.3 nm s^{-1} for Te. The thickness of each layer was selected to achieve the atomic ratio $In/(Se+Te) \approx 2/3$, while the Se/Te atomic ratio was 50/15. In fact, since during the annealing there is some chalcogen loss, the ratio is slightly smaller than 2/3. The thicknesses of the layers varied from 10 nm to 30 nm. A last selenium layer was deposited by evaporation (100 nm) to protect the underlayers from oxidation during transfer from the deposition apparatus to the oven for the post-annealing treatment. The $In_2Se_{3-3x}Te_{3x}$ samples were synthesized by a solid-state reaction, induced by annealing.

The total thicknesses of the films were checked using a mechanical finger.

After deposition, the multilayer structures were annealed in an open Pyrex tube put in a tubular oven under an argon flow (30 l h^{-1}). The heating temperature varied from 620 to 720 K and the annealing time was half an hour.

The Se deposited at the surface of the sample to prevent its oxidation is evaporated during the annealing, as shown by the Se condensation onto the cold extremity of the Pyrex tube.

2.2. Thin-film characterization

The structure of the films was examined using an x-ray goniometer. The full width at half-maximum (FWHM) of the diffraction peaks was used to estimate the grain size [6]. The surface morphology and the cross section were observed with a field-effect scanning electron microscope JEOL 6400F; quantitative analyses were performed by electron probe microanalysis (EPMA). Surface and near-surface quantitative analyses were also performed using x-ray photoelectron spectroscopy (XPS). The XPS quantitative analyses were based on the determination of the In $3d_{5/2}$, Se 3d and Te $3d_{5/2}$ peaks with 3.8, 0.57 and 5.4, respectively, as the sensitivity factors given by the manufacturer (Leybold). The oxygen contamination was determined by recording successive XPS spectra obtained after ion etching for short periods. Using an ion gun, sputtering was accomplished at pressures of less than 5×10^{-4} Pa with a 10 mA emission current and 5 kV beam energy. The Ar^+-ion beam was rastered over the entire sample surface. At the surface of the films, there is carbon contamination. In the apparatus used, the C–C bond has a well defined position at 284.4 eV and the carbon peak was used as a reference to estimate the electrical charge effect, as the film substrates were insulating glass.

The optical measurements were carried out at room temperature using a Cary spectrophotometer. The optical density was measured at wavelengths from 2000 nm to 300 nm with a step of 5 nm.

The photoconductivity was measured at room temperature in the range 400 to 800 nm using a transverse arrangement. A HUET M 25 monochromator and a tungsten lamp provided the incident radiation. A radiometer, PHOTODYNE 88 XLA, was used in order to obtain a constant light flow when the energy was varied.

3. Results

For comparison, γ-In_2Se_3 reference samples have been grown [3]. They have been synthesized following the same process as described above, the only difference being the lack of tellurium in the sequentially deposited samples.

As the compounds studied, $In_2Se_{3-3x}Te_{3x}$, are obtained by post-annealing of sequentially deposited In/Se/Te/$\cdots$ layers, many parameters can be modified, such as the at.% Te/at.% Se deposition ratio, annealing time and annealing temperature. All of these can modify the final film composition and properties. Therefore, for simplicity, only the annealing temperature was varied, which allows us to see its influence clearly. It was shown earlier [3, 4, 7] that films with optimum performance are obtained for an annealing duration of half an hour. The starting atomic ratio percentage Te/(In + Se + Te) has been chosen to be 15 at.%, since it has been checked that when the present one-step annealing process is used, homogeneous films cannot be obtained for higher atomic concentration. The parameter chosen is the annealing temperature, which was varied from 620 to 720 K.

3.1. EPMA and XPS quantitative analyses

The averaged composition of the samples before annealing has been estimated. The samples contain around 15 at.% of Te before annealing. After annealing, the Te/Se atomic ratio varies with the annealing temperature, while the stoichiometric ratio indium/chalcogen $= 2/3$ is systematically obtained (table 1). The oxygen contamination in the film is so small that it cannot be quantified. The XPS quantitative analysis, which is a surface analysis, is reported in table 2. Also reported are the results after 1, 2, 3 and 6 min of etching, measured in order to estimate the near-surface composition. Since similar results are obtained for each of the films, only the results obtained for annealing at 720 K are reported. It can be seen that, at the surface and near the surface, the films are chalcogen deficient, while there is some oxygen surface contamination.

Of course, the sputtering yields of the different atoms are certainly different, and the XPS quantitative analysis should be considered only as indicative of a tendency.

Table 1. EPMA quantitative analysis.

		Atomic percentage			
		In	Se	Te	O
Before annealing		35	50	15	0
Annealing	620	40	52	8	0
temperature	670	40	58.5	1.5	0
(K)	720	40	59.2	0.8	0
In_2Se_3 reference		40	60	0	0

Table 2. XPS quantitative analysis of a film annealed at 670 K.

Etching time (min)	In (at.%)	Se (at.%)	Te (at.%)	O (at.%)
0	20	24	1	55
*	48	50	2	—
1	41.5	48	0.5	10
*	45.5	53.5	1	—
3	44	50	0.5	5.5
*	46.5	53	0.5	—
6	47.5	52	0.5	—

* Second line: approximate composition given as the atomic percentage of the ternary compound.

3.2. Structural and morphological study

Figure 1 shows a typical XRD pattern of a thin film annealed at 620 K. The results obtained for the different annealing temperatures are not very different; however, there is some modification of the preferential orientation of the crystallites. This preferential orientation along the (00*l*) direction increases with the Te content in the films (table 3). The peaks were identified by comparing (table 4) the *d*-values obtained from the XRD patterns with the standard reference of γ-In_2Se_3 (JCPDS file No 40-1407). The alloy $In_2Se_{3-3x}Te_{3x}$ crystallizes in the hexagonal structure of γ-In_2Se_3. The averaged grain size has been estimated using the FWHM method. With this method, the grain size in the direction perpendicular to the plane of the substrate can be estimated from the width of the diffraction peak. However, this technique cannot be used for measurements of grains larger than 150–200 nm since, in that case, the width at half-maximum of the diffraction peak is similar to that of the reference powder, which is the case in the present work (table 3).

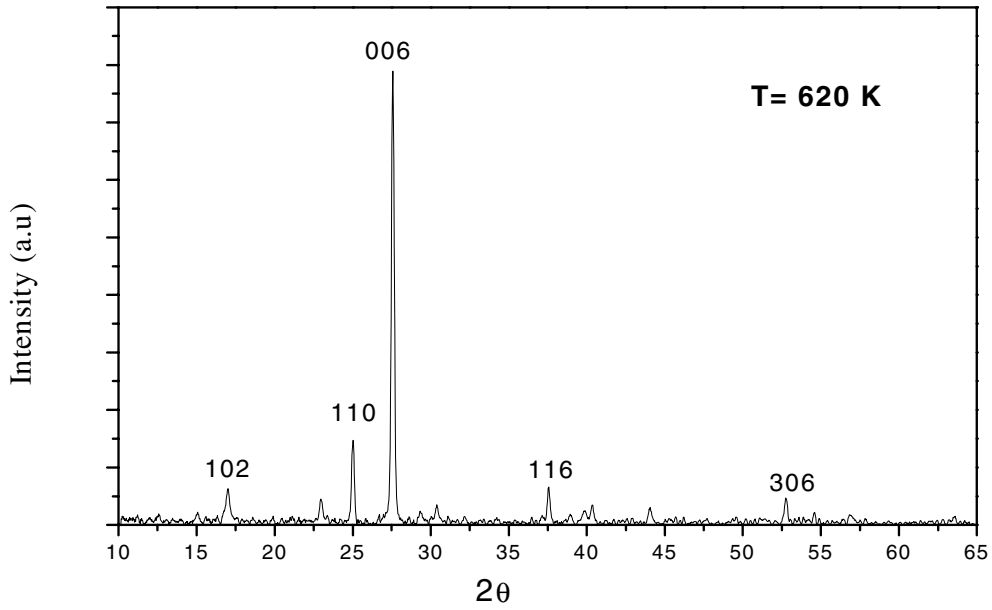

Figure 1. An x-ray diagram of an $In_2Se_{3-3x}Te_{3x}$ film annealed at 620 K for half an hour.

Table 3. Synthesis of the physico-chemical and optoelectrical characterization.

	Annealing temperature/Te at.%		
	620/8	670/1.5	720/0.8
a (nm)	0.7138	0.7138	0.7140
c (nm)	1.9470	1.9458	1.9488
$F(00l)$	0.67	0.63	0.56
FWHM (deg)	0.2169	0.1985	0.1928
E_g (eV)	1.8	1.81	1.81
$E_{g,ph}$ (eV)	1.758	1.76	1.75

Table 4. Comparison of the d-values of films with different x and JCPDS data (40-1407).

	γ-In_2Se_3 JCPDS data	$In_2Se_{3-3x}Te_{3x}$ Annealing temperature (in K)		
	40-1407	620	670	720
$d(006)$ (nm)	0.32308	0.3245	0.3243	0.3248
$d(110)$ (nm)	0.35635	0.3569	0.3569	0.3570

The surface morphology of the films has been observed by SEM (figures 2 and 3). It can be seen in figure 2(a) that the films are homogeneous, while in figure 2(b) grains are clearly visible with an average size of 200 nm. Grains are also clearly visible in the cross section of figure 3. The thickness of the grains visible in the micrographs varies between 200 and 300 nm, which is in good agreement with the FWHM method.

It can also be seen that there is a good adherence of the films to the glass substrate.

3.3. Optoelectrical characterization

A typical transmission voltage curve is presented in figure 4. Interference fringes are clearly visible in the domain of high transmission. The absorption threshold voltage is situated at about 680 nm, which allows a first rough estimation of the optical gap of about 1.8 eV.

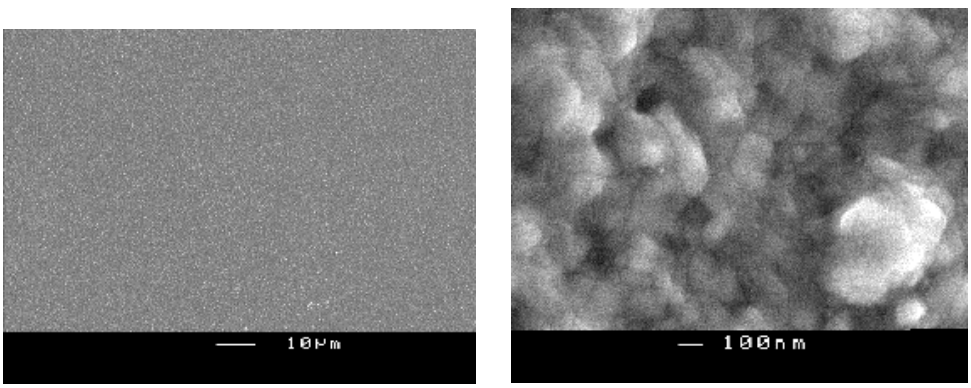

(a) (b)

Figure 2. A micrograph of an $In_2Se_{3-3x}Te_{3x}$ film annealed at 620 K half an hour: (a) small magnification; (b) large magnification.

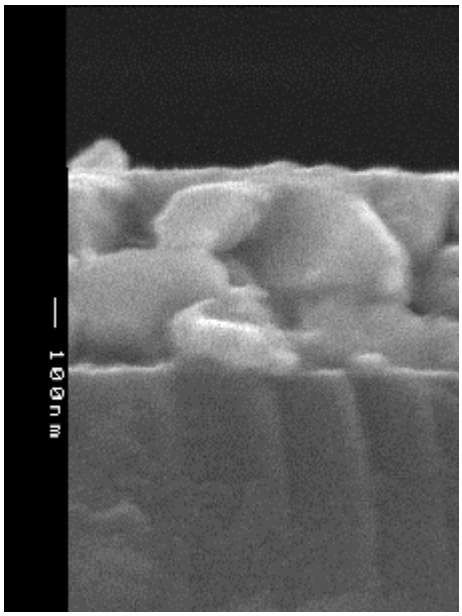

Figure 3. A cross section image of an $In_2Se_{3-3x}Te_{3x}$ film—deposited on glass—annealed at 620 K for half an hour.

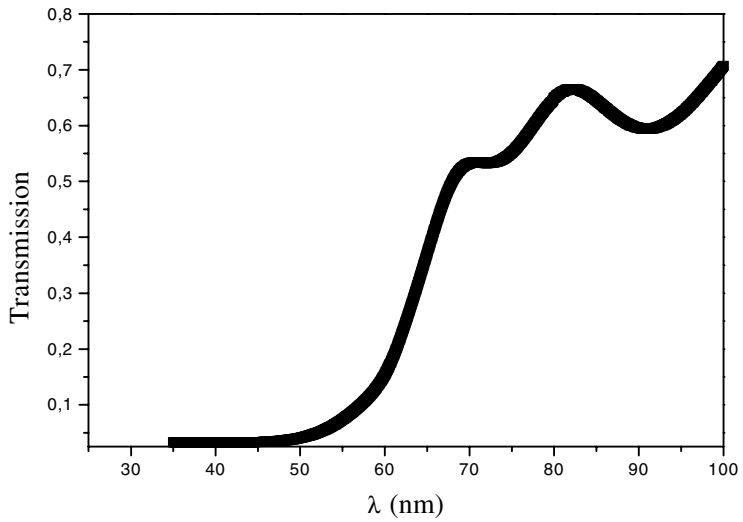

Figure 4. Transmission coefficient versus wavelength of the incident light for an $In_2Se_{3-3x}Te_{3x}$ film annealed at 620 K for half an hour.

The variations of the photoconductivity with the wavelength for three typical samples are reported in figure 5. It can be seen that they have similar shapes with a turn-on wavelength of the photocurrent at about 685 nm. However, while the shape is similar, the scale of the photocurrent is not the same when x varies. The light effect is more than five orders of magnitude higher when $x = 8$ at.% than for the other samples, i.e. when the tellurium concentration is low.

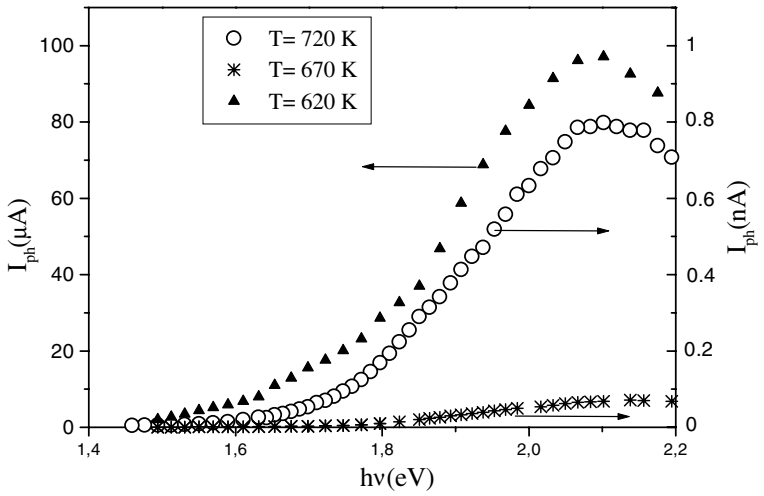

Figure 5. Photoconductivity versus wavelength for $In_2Se_{3-3x}Te_{3x}$ film.

4. Discussion

It can be seen that while the films show chalcogen excess after deposition, they are stoichiometric after annealing, which means that there is some chalcogen loss during the synthesis process. It can be seen, also, that the tellurium atomic concentration in the films decreases when the annealing temperature increases; moreover, the Te/Se ratio decreases systematically during the annealing, which means that tellurium leaves the film faster than selenium, and that this difference increases with the temperature. The chalcogen-loss effect is corroborated by the XPS analysis. At the surface, the films are strongly chalcogen deficient. However, it can be deduced from table 2 that this effect is only a surface effect since, while the etching rates of chalcogen are higher than those of metals [8], the relative atomic concentration of chalcogen increases upon etching, which shows that there is a positive gradient of the chalcogen concentration in the under-surface layer. This justifies the claim that the films are stoichiometric in the bulk, while they are chalcogen deficient at the surface. During the annealing, the thermal energy induces two opposite phenomena:

- chalcogens have high vapour pressure, which induces their migration toward the surface from where they leave the sample;
- chalcogens react with indium to give the stable compound $In_2Se_{3-3x}Te_{3x}$.

Since the vapour pressure of selenium is higher than that of tellurium, it might be thought that it should leave the film faster than tellurium. However, the kinetics of the chemical reaction and the stability of the different chalcogen compounds should be taken into account.

We showed earlier that, while selenium compounds are very stable [9], tellurium compounds are not [10]. We have also shown that in the case of competition between tellurium and selenium during post-annealing of thin films, the selenium is substituted for tellurium [11]. This effect can be explained by the electronegativity values of Te ($\chi_{Te} = 2.1$) and Se ($\chi_{Se} = 2.4$) [12]. The electronegativity difference between the metal (here In, with ($\chi_{In} = 1.7$)) and the chalcogen controls the kinetics of the reaction and the stability of the chalcogenide compounds. Therefore, since $\chi_{Se} - \chi_{In} = 0.7$ and $\chi_{Te} - \chi_{In} = 0.4$, the selenide compound is more stable and easier to synthesize than the telluride compounds.

In the same field, it can be seen in figure 6 that while the shape of the Se 3d signal does not change upon etching, that of tellurium is strongly modified.

Before etching, two doublets are visible. The decompositions of these peaks are presented in figure 7 (Se 3d) and figure 8 (Te 3d). It can be seen that just one doublet is sufficient to fit the experimental curve in the case of Se, while two doublets are necessary in the case of Te. The one with Te $3d_{5/2} = 576$ eV corresponds to TeO_2 [13] while the other one, at 573 eV, can be attributed to the $In_2Se_{3-3x}Te_{3x}$ compound. If the Te signal intensity of oxidized Te is I_{ox} and that of metallic Te is I_m, the thickness of the oxide at the surface of the film may be deduced from the I_{ox}/I_m ratio. Since the growth of TeO_2 in air is homogeneous, the oxide thickness d

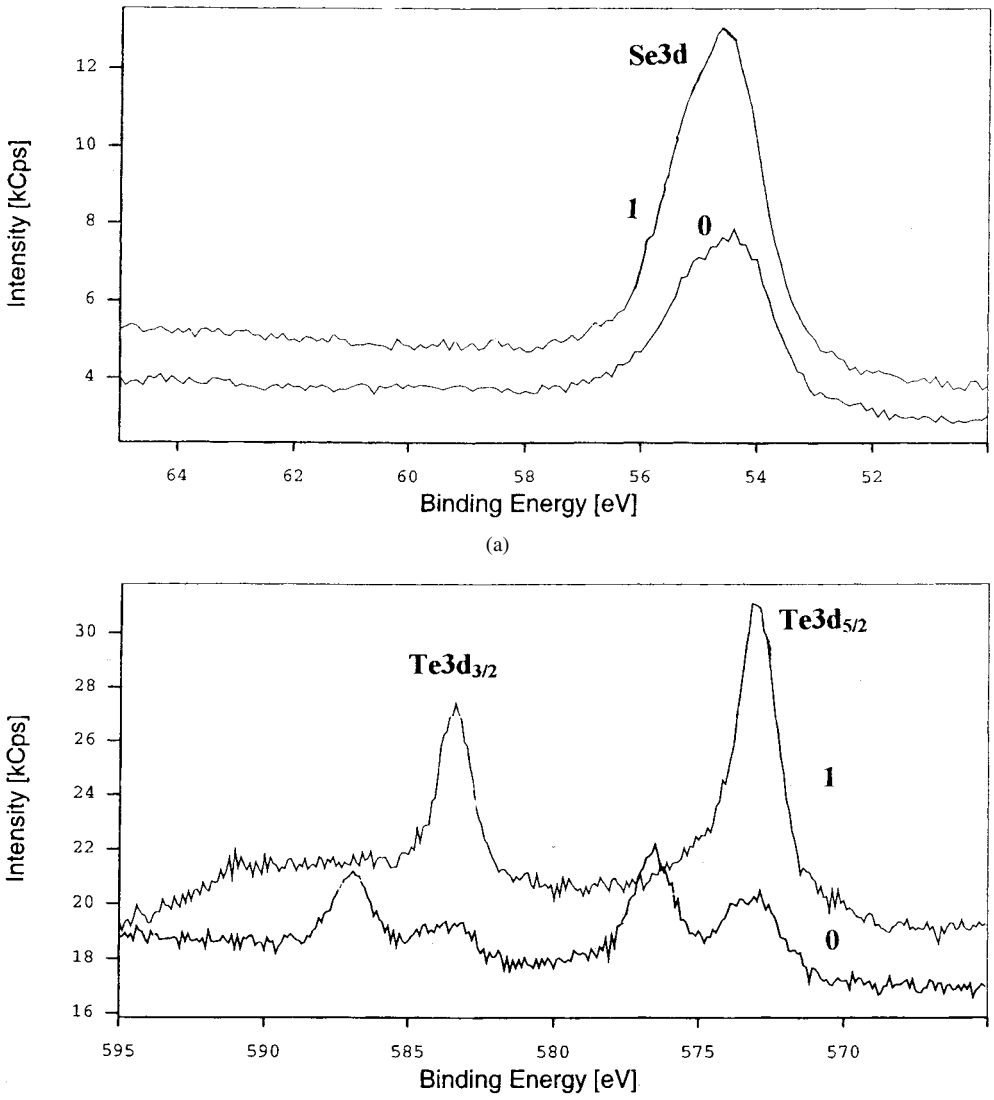

Figure 6. The XPS chalcogen peak at the surface and after 1 min of etching of an $In_2Se_{3-3x}Te_{3x}$ film annealed at 620 K for half an hour. (a) Se 3d. (b) Te 3d.

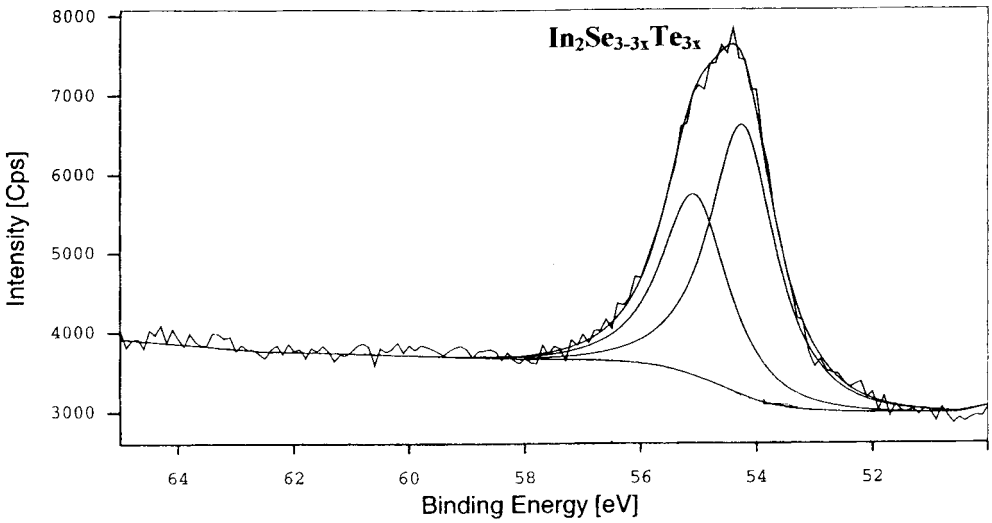

Figure 7. Decomposition of the Se 3d peak.

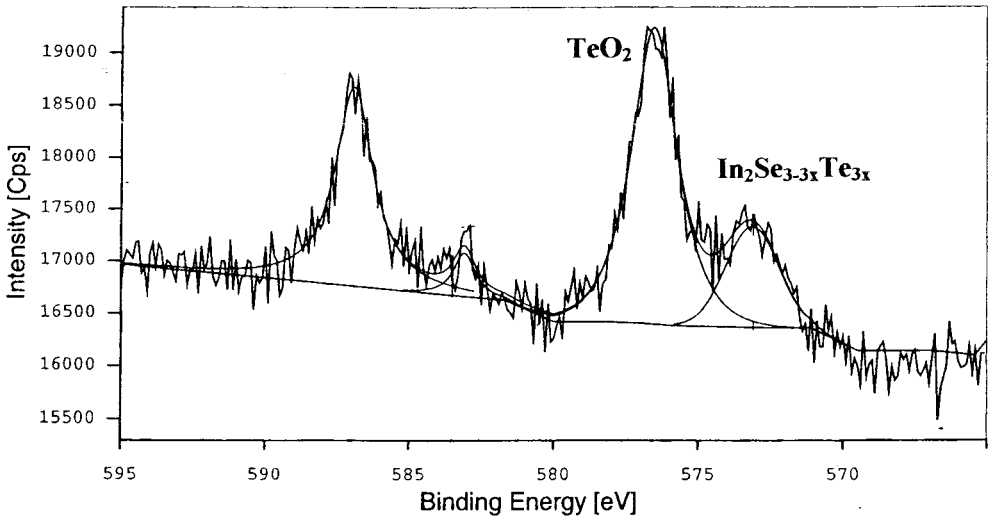

Figure 8. Decomposition of the Te 3d peak.

is related to I_{ox}/I_m by [14]

$$d = \lambda \cos(\theta) \ln\left[\left(1 + \frac{\rho_m}{\rho_{ox}}\right)\left(\frac{I_{ox}}{I_m}\right)\right]$$

where λ is the mean electron escape depth in TeO_2 ($\approx$0.5 nm for TeO_2 electrons), the take-off angle θ is 0° for the spectrometer used and ρ_m and ρ_{ox} are the atomic densities of Te and TeO_2, equal to 2.8×10^{23} and 2.2×10^{23} cm^{-3}, respectively. The oxide thickness is calculated to be around 1 nm.

This superficial oxidation of tellurium, not shown by selenium, confirms the higher stability of the selenide compounds.

The lattice parameters calculated from the experimental values reported in table 4 are presented in table 3. Since the lattice parameters of γ-In_2Se_3 given in the references are $a = 0.7128$ nm and $c = 1.9382$ nm, it can be said that in the concentration range studied here, there is no visible evolution of the lattice parameters with the Te concentration. It should be noted that there is no γ-phase of In_2Te_3 (only α- and β-phases) and that this compound is systematically cubic, unlike γ-In_2Se_3, which is hexagonal. The Vegard law, which describes the transition, with varying composition, from the lattice constants of one compound to those of the other, cannot apply here. Therefore, the hexagonal structure of γ-In_2Se_3 will only be preserved for small tellurium concentration, while when the concentration increases, other phases will be present in the film (α-In_2Te_3). Up to this limit, the tellurium will induce strains and faults in the films which explain the small discrepancy between the calculated lattice parameters and the expected ones.

It can be seen in table 3 that the FWHM of the x-ray diffraction peaks decreases with the increasing temperature, which means that the grain size increases. However, the orientation of the crystallites decreases with the increase of the annealing temperature; this could be attributable to the fact that tellurium induces film orientation.

The transmittance spectrum of a film with a thickness of 650 nm is presented in figure 4; it has been taken at room temperature. The interference fringes visible in the spectrum corroborate the high morphological quality of the films; their surfaces are smooth and parallel.

Manifacier *et al* [15] have shown that the real part of the refractive index n can be deduced from the fringe pattern of the transmission spectrum. They have shown that at a given wavelength λ, n is given by

$$n = [N + (N^2 - n_s^2)^{1/2}]^{1/2}$$

where

$$N = [(1 + n_s^2)/2] + 2n_s[T_{max} - T_{min}]/(T_{max}T_{min})$$

where n_s is the refractive index of the substrate, T_{max} is the maximum transmission, T_{min} is the minimum transmission.

T_{max} and T_{min} are considered as continuous functions of λ; they are the envelopes of the maxima and the minima in the transmission spectrum.

In the present case, for $In_2Se_{3-3x}Te_{3x}$, $n = 2.5$ at $\lambda = 1000$ nm, which is similar to the value measured by us for γ-In_2Se_3 thin films at $\lambda = 800$ nm [3].

The absorption coefficient α has been calculated from the measurements of the transmission T of two samples (1 and 2) of different thicknesses (t) [16]:

$$\alpha = \frac{1}{t_2 - t_1} \log \frac{T_1}{T_2}.$$

Any errors present in the values of the uncertainties obtained by this technique are much less than the errors in the thickness measurements, which dominate the experimental errors. In the 1.6–2.3 energy range, α varies from 10^4 cm^{-1} to 10^5 cm^{-1}, which is very promising for photovoltaic applications. The band gap has been estimated from these measurements. γ-In_2Se_3 is a direct-band-gap semiconductor. A typical $(\alpha h\nu)^2 = f(h\nu)$ curve is presented in figure 9. The optical band gap was estimated by extrapolating the straight lines of $(\alpha h\nu)^2$ versus $h\nu$. It can be seen in table 3 that it is around or slightly higher than 1.8 eV. This value corresponds to that expected for pure γ-In_2Se_3. The same values have been obtained by using the $(I_{ph})^2$ versus $h\nu$ curves (figure 10, table 3). There is no clear relation between the tellurium atomic concentration and the gap value. It can be concluded that the empirical law described by Hill [17] is not respected. Here also the lack of γ-In_2Te_3 phase can explain such a discrepancy.

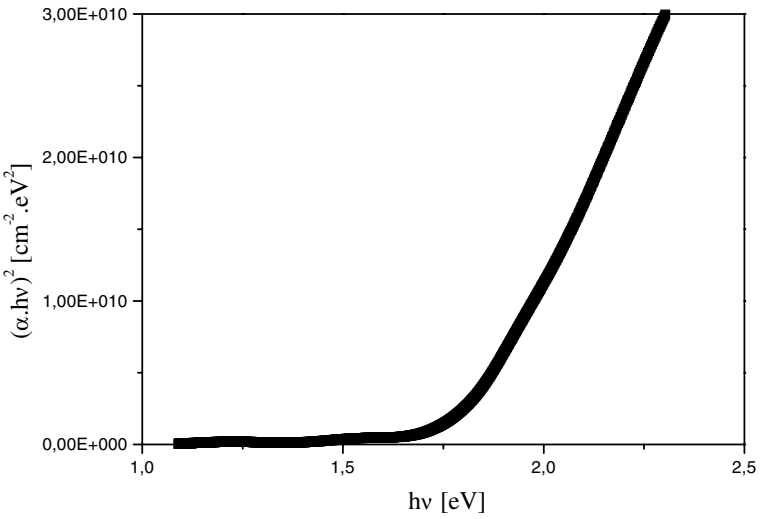

Figure 9. $(\alpha h\nu)^2 = f(h\nu)$.

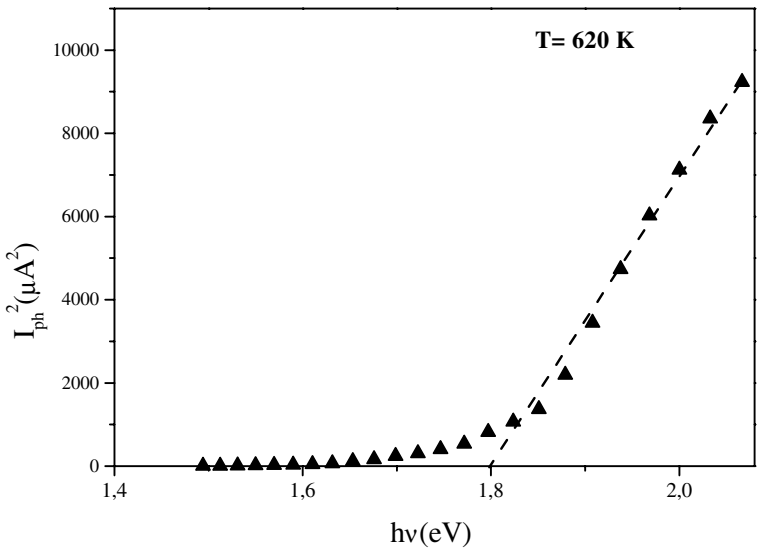

Figure 10. $I_{ph}^2 = f(h\nu)$.

Moreover, it has been shown that in MS:X 'alloys', the influence of tellurium is very different to that of selenium [18].

In the case of Se (CdS:Se, ZnS:Se), the alloys follow a classical evolution of the lattice parameters and optical gap, i.e. in these alloys the band edges shift as a whole as the alloy composition increases, because the chalcogen atoms are isovalent and there is no defect energy level induced in the gap. This is not the case with tellurium, because in that case the two constituents in the alloy have very different atomic potentials and atomic sizes; localized isovalent defect states can exist inside the band gap, leading to abrupt changes in the alloy optical properties for high impurity concentrations. Such different isovalent levels have

been observed in mixed-anion systems (ZnS:Te, CdS:Te). Thus, a small amount of Te in $In_2Se_{3-3x}Te_{3x}$ could have significant effects on its properties, such as its photoconductivity. Therefore such a level induced in the band gap could explain the strong enhancement of the photoconductivity current.

5. Conclusions

$In_2Se_{3-3x}Te_{3x}$ films have been synthesized by post-annealing of In/Se/Te/$\cdots$ sequentially deposited films. The main result obtained is the strong enhancement of the photoconductivity current, since for 8 at.% of Te the magnitude of the photocurrent is five orders of magnitude higher than for pure γ-In_2Se_3.

We have shown that the alloy properties follow neither the Vegard law nor the Hill law. This is explained by the large difference in atomic potential and atomic size between Se and Te. By analogy with MS:Te compounds, we propose that in that case, the tellurium acts as a isoelectronic trap in the gap. Calculations are now under way to estimate the energy position of the level induced in the gap in order to check the above hypothesis.

References

[1] Contreras M A, Egaas B, Ramanathan K, Hiltner J, Swartlander A, Hasoon F and Noufi R 1999 *Prog. Photovolt. Res. Appl.* **7** 311
[2] Nadenau V, Rau U, Jasenek A and Schock H W 2000 *J. Appl. Phys.* **87** 584
[3] Marsillac S, Bernède J C, Emziane M, Wery J, Faulques E and Le Ray P 1999 *Appl. Surf. Sci.* **151** 171
[4] Bernède J C, Marsillac S and Conan A 1997 *Mater. Chem. Phys.* **48** 5
[5] Agnihotrio P and Raturi A K 1983 *Thin Solid Films* **108** 313
[6] Kaeble E F 1967 *Handbook of X-Rays* (New York: McGraw-Hill)
[7] Gourmelon E, Hadouda H, Bernède J C and Pouzet J 1997 *Vacuum* **48** 509
[8] Bernède J C 2001 *Appl. Surf. Sci.* **171** 15
[9] Pouzet J, Hadouda H, Bernède J C and Le Ny R 1996 *J. Phys. Chem. Solids* **57** 1363
[10] Kettaf M, Conan A, Bonnet A and Bernède J C 1990 *J. Phys. Chem. Solids* **51** 333
[11] Pouzet J, Bernède J C and Ouadah A 1993 *Phys. Status Solidi* a **139** 471
[12] Bernède J C and Pouzet J 1994 *Le Vide. Les Couches Minces* **270** 1
[13] Beamon G and Briggs D 1993 *High Resolution XPS of Organic Polymers. The Scienta ESCA 300 Data Base* (Chichester: Wiley)
[14] Lee Wen Young and Geiss R H 1983 *J. Appl. Phys.* **54** 1351
[15] Manifacier J C, Gasiot J and Fillard J P 1976 *J. Phys. E: Sci. Instrum.* **9** 1002
[16] Bischel R and Levy F 1985 *Thin Solid Films* **124** 75
[17] Hill R 1974 *J. Phys. C: Solid State Phys.* **7** 521.
[18] Wei S H, Zhang S B and Zunger A 2000 *J. Appl. Phys.* **87** 1304